PLOS | ONE

RESEARCH ARTICLE

Solution Structural Studies of GTP: Adenosylcobinamide-Phosphateguanylyl Transferase (CobY) from *Methanocaldococcus jannaschii*

Kiran K. Singarapu[1,2]*, Michele M. Otte[3¤], Marco Tonelli[1], William M. Westler[1], Jorge C. Escalante-Semerena[3], John L. Markley[1]*

1 National Magnetic Resonance Facility at Madison and Department of Biochemistry, University of Wisconsin-Madison, Madison, Wisconsin, United States of America, **2** Center for NMR and Structural Chemistry, CSIR-Indian Institute of Chemical Technology, Tarnaka, Hyderabad, Telangana, India, **3** Department of Microbiology, University of Georgia, Athens, Georgia, United States of America

¤ Current address: Lonza Specialty Ingredients, Alpharetta, Georgia, United States of America
* singarapu@iict.res.in (KKS); jmarkley@wisc.edu (JLM)

OPEN ACCESS

Citation: Singarapu KK, Otte MM, Tonelli M, Westler WM, Escalante-Semerena JC, Markley JL (2015) Solution Structural Studies of GTP: Adenosylcobinamide-Phosphateguanylyl Transferase (CobY) from *Methanocaldococcus jannaschii*. PLoS ONE 10(10): e0141297. doi:10.1371/journal.pone.0141297

Editor: Eugene A. Permyakov, Russian Academy of Sciences, Institute for Biological Instrumentation, RUSSIAN FEDERATION

Received: July 20, 2015

Accepted: October 7, 2015

Published: October 29, 2015

Data Availability Statement: The protein coordinates were deposited in the Protein Data Bank (PDB) with accession code 2MZB, and the chemical shifts were deposited in Biological Magnetic Resonance Data Bank (BMRB) with accession code 25482.

Funding: This work was supported by National Institutes of Health (NIH) Grants R37 GM040313 to JCE-S and P41 GM103399 to JLM, which supports the National Magnetic Resonance Facility at

Abstract

GTP:adenosylcobinamide-phosphate (AdoCbi-P) guanylyl transferase (CobY) is an enzyme that transfers the GMP moiety of GTP to AdoCbi yielding AdoCbi-GDP in the late steps of the assembly of Ado-cobamides in archaea. The failure of repeated attempts to crystallize ligand-free (apo) CobY prompted us to explore its 3D structure by solution NMR spectroscopy. As reported here, the solution structure has a mixed α/β fold consisting of seven β-strands and five α-helices, which is very similar to a Rossmann fold. Titration of apo-CobY with GTP resulted in large changes in amide proton chemical shifts that indicated major structural perturbations upon complex formation. However, the CobY:GTP complex as followed by ^{1}H-^{15}N HSQC spectra was found to be unstable over time: GTP hydrolyzed and the protein converted slowly to a species with an NMR spectrum similar to that of apo-CobY. The variant CobY^{G153D}, whose GTP complex was studied by X-ray crystallography, yielded NMR spectra similar to those of wild-type CobY in both its apo- state and in complex with GTP. The CobY^{G153D}:GTP complex was also found to be unstable over time.

Introduction

Coenzyme B_{12} (a.k.a. adenosylcobalamin or AdoCbi) is the largest, non-polymeric molecule with biological activity. AdoCbi belongs to the broadly distributed family of cyclic tetrapyrrole molecules known as 'The Pigments of Life', which includes hemes, factor F_{430}, and chlorophylls [1]. The core ring structure of AdoCbi (a.k.a. the corrin ring) contains a cobalt ion chelated by pyrrolic nitrogens. On the upper (beta) face of the ring, a covalent bond links 5′-deoxyadenosine (Ado) and the Co ion. This unique organometallic bond is critical to the function of the coenzyme. The lower (alpha) face of the ring features a nucleotide loop tethered to a

Madison. KKS received support from a Ramanujan Fellowship from the Department of Science and Technology (DST-India).

Competing Interests: The authors have declared that no competing interests exist.

Abbreviations: Apo-CobY, wild-type, ligand-free CobY; CobY^{G153D}, G153D variant of CobY; BMRB, Biological Magnetic Resonance Data Bank; DTT, dithiothreitol; HSQC, heteronuclear single-quantum coherence; NMR, nuclear magnetic resonance; NOE, nuclear Overhauser enhancement; NOESY, NOE spectroscopy; PDB, Protein Data Bank; rmsd, root mean square deviation; τ_c, rotational correlation time; TALOS, torsion angle likelihood obtained from shifts.

substituent of the ring *via* a phosphodiester bond. Two features unique to the nucleotide loop are the alpha-*N*-glycosidic bond between the base and ribosyl moiety, and the diversity in the base [2]. 'Cobamide' is the term used to refer to complete B_{12}-like molecules, regardless of their base. The best known cobamide is cobalamin, which contains 5,6-dimethylbenzimidazole as its base.

The assembly of the nucleotide loop evolved differently in bacteria and archaea. In both domains, the pathway starts with the synthesis of AdoCbi-P, which is then converted to AdoCbi-GDP, the so-called activated corrin ring. The difference between the way archaea and bacteria synthesize AdoCbi-GDP lies in the guanylyl transferase that transfers the GMP moiety of GTP to AdoCbi-P. Bacteria use a bi-functional kinase/guanylyl transferase enzyme (CobU, EC 2.7.7.62) [3–5], whilst archaea evolved CobY (E.C. 2.7.7.62), a guanylyl transferase that lacks kinase activity [6]. Crystal structures of CobU in its apo form and in complex with GMP are available (PDB 1C9K [5] and 1CBU [7], respectively). The crystal structure of CobY^{G153D} in complex with GTP is also available (PDB 3RSB) [8], but efforts to crystallize the apo-forms of CobY or CobY^{G153D} were unsuccessful.

Results of biochemical experiments performed during the course of this work revealed that two subunits of apo-CobY bind one GTP molecule with a binding constant of $K_b = 2.0 \times 10^{-5}$ M^{-1} and a dissociation constant of $K_d = 5.0 \times 10^{-6}$ M, but apo-CobY failed to bind GTP analogues, such as GMP-PNP, GMP-PCP or even GDP [9]. CobY binds GTP first before binding AdoCbi-P 200 [9]. The Ado moiety of the corrinoid is required for binding, but the order of binding is clear. The G153D variant of CobY (CobY^{G153D}) crystallized in the presence of GTP and led to the determination of the 3D structure of the complex by X-ray crystallography at a resolution of 2.8 Å [8]. Repeated failed attempts to crystallize the apo-CobY protein prompted us to explore solution NMR spectroscopy as a means for determining the structure of apo-CobY and its complex with GTP. To aid in answering how CobY binds GTP and is involved in transferring the GMP moiety to AdoCbi-P, we conducted structural studies using nuclear magnetic resonance (NMR) spectroscopy. We report here the solution structure of apo-CobY, which has allowed comparison with the X-ray structure of CobY^{G153D}. We also present NMR studies of CobY^{G153D} and interactions of the proteins with GTP.

Materials and Methods

Protein production and sample preparation

[U-^{15}N]-CobY, [(U-^{13}C, ^{15}N]-CobY, and [U-^{13}C, ^{15}N]-CobY^{G153D} protein samples containing 196 amino acids (residues 1–196) used NMR studies were produced in minimal medium according to the protocol described previously [10], except that *E. coli* BL21-CodonPlus® (DE3)-RIL (Stratagene)was used for protein production, and cultures were grown in Erlenmeyer flasks. The *M.jannaschiicobY* gene was expressed from plasmid pCobY14 [9]. Proteins were purified as previously reported [9] with the following modifications. Cell-free extract was applied to a 5 mL HiTrap phenyl (high-sub) FF column (GE Healthcare) equilibrated with tris (hydroxymethyl) aminomethane hydrochloride buffer (50 mM Tris-HCI, pH 8.0 at 4°C) containing 55 g/L $(NH_4)_2S0_4$. Protein was eluted at a flow rate of 5 mL / min with a linear gradient to 100% Tris-HCI buffer. CobY-containing fractions were concentrated and dialyzed against Tris-HCI buffer. Protein purity was assessed as previously reported [9] and found to be >95% homogeneous (data not shown). Ion exchange chromatography was therefore omitted. [U-^{13}C, ^{15}N]-CobY protein used for structure determination was further dialyzed against 50 mM deuterated Tris buffer (pH 8.0 at 4°C) containing 50mM NaCl, 5 mM dithiothreitol (DTT) and 10 mM $MgCl_2$. To prevent bacterial growth, 0.2% NaN_3 was added to all samples and proteins were stored at 4°C.

NMR Data Collection and Analysis

All NMR spectra were recorded at the National Magnetic Resonance Facility at Madison (NMRFAM) on Varian VNMRS (600 MHz, 800 MHz and 900 MHz) spectrometers equipped with triple-resonance cryogenic probes. The temperature of the sample was regulated at 40°C. Sequence specific backbone resonance assignments were conducted for CobY using a series of 2D and 3D heteronuclear NMR spectra. NMR data were collected for both CobY containing 2.0 mM [U-^{13}C,^{15}N] protein dissolved in NMR buffer with 50 mM Tris, 5 mM DTT, 50 mM NaCl, 10 mM $MgCl_2$,95% H_2O, 5% D_2O. Raw NMR data were processed with NMRPipe [11] and analyzed using the programs XEASY [12] and NMRFAM-SPARKY [13]. 2D ^{1}H-^{15}N HSQC and 3D HNCO data sets were used to identify the number of spin systems, and these identifications plus 3D HNCACB and 3D CBCA(CO)NH data sets were used as input to the PINE server [14] to determine sequence specific backbone resonance assignments. In addition, backbone resonance assignments were confirmed on the basis of 3D ^{15}N-edited ^{1}H-^{1}H 3D-NOESY. 2D ^{1}H-^{13}C HSQC, 3D HBHA(CO)NH, 3D HC(CO)NH, 3D C(CO)NH experiments were used to assign the side chain and HB and HA resonances. 3D ^{15}N-edited ^{1}H-^{1}H NOESY (100 ms mixing time), and 3D ^{13}C-edited ^{1}H-^{1}H NOESY (120 ms mixing time) experiments were used to derive the distance constraints to determine the three dimensional structure of protein [15]. Standard pulse sequences were used to record steady state [^{1}H]-^{15}N NOE and ^{15}N relaxation (T_1, T_2) data [16]. To determine the ^{15}N T_1 values, multiple interleaved NMR spectra were recorded with relaxation delays of 10, 100, 200, 400, 600, 800, 1000, 1200, and 1400 ms. To determine ^{15}N T_2 values, multiple interleaved NMR spectra were recorded with delays of 10, 30, 50, 70, 90, 110, and 150 ms. Relaxation rates were calculated by least-squares fitting of peak heights versus relaxation delay to one single exponential decay by using NMRFAM-SPARKY. The reported error estimates are standard deviations derived from fitting the data. Steady-state [^{1}H]-^{15}N NOE values were calculated from the ratio of peak heights in a pair of NMR spectra acquired with and without proton saturation. The signal-to-noise ratio in each spectrum was used to estimate the experimental uncertainty.

Structure calculation and analysis

For the structure calculation, ^{15}N resolved ^{1}H-^{1}H 3D NOESY and ^{13}C resolved ^{1}H-^{1}H 3D NOESY spectra were used to derive the intra molecular distance restraints. TALOS+ software [17] was used to derive backbone dihedral angle restraints φ and ψ from ^{1}H, ^{15}N, ^{13}CA, ^{13}CB, $^{13}C'$chemical shifts. CYANA (version 3.0) [18] was used for automated NOESY peaks assignments and structure calculation. NOESY peaks assigned automatically by CYANA were used as a guide to further refine the structure. Programs MOLMOL [19] and PYMOL [20] were used, respectively, to calculate the root mean square deviation (rmsd) and for graphical analysis. The PSVS server [21] was used to check the quality of the structure.

Results and Discussion

Optimization of NMR sample conditions

By optimizing the buffer composition and temperature, we discovered conditions that led to sharp and uniform signals in the ^{1}H-^{15}N HSQC spectrum (Fig 1A) and good triple-resonance and NOESY data, as needed for a successful structure determination. The final conditions were:2 mM protein in 50 mM TRIS buffer pH 7.0 containing 50 mM NaCl and 10 mM$MgCl_2$. Data were collected at 40°C.

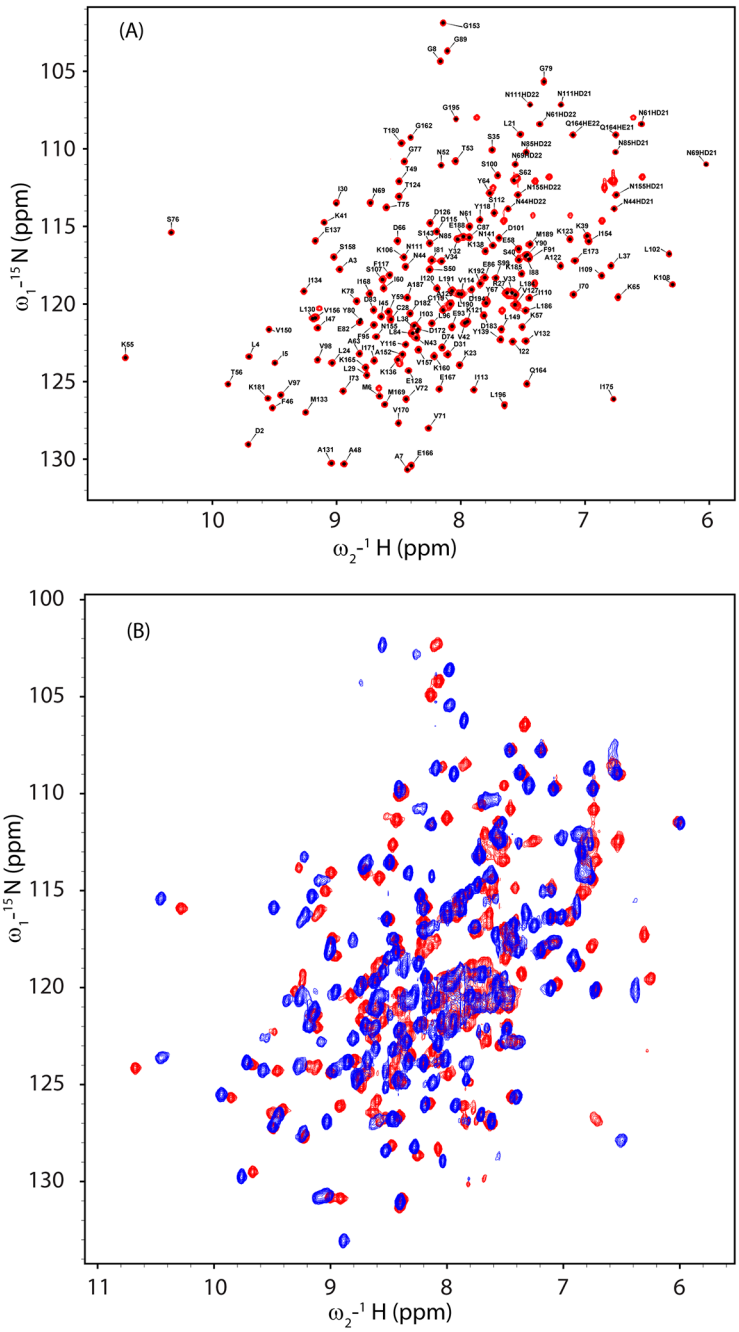

Fig 1. 2D ^{1}H-^{15}N NMR Spectra of CobY and its GTP Complex. (A) ^{1}H-^{15}N HSQC spectrum of apo-CobY. Amide peaks are labeled with their residue assignments. (B) Overlay of the ^{1}H-^{15}N HSQC spectrum of apo-CobY (red) with that of the CobY:GTP complex (blue).

doi:10.1371/journal.pone.0141297.g001

Structure of apo-CobY

The solution NMR structure of apo-CobY was determined from 3246 distance constraints from NOESY spectra and 220 angle constraints derived from chemical shifts by using the TALOS+ program [17]. Two hundred refined structures were generated, and the best 20 conformers, those with lowest energy that showed the fewest constraint violations with CYANA

[18], were chosen for additional water bath refinement using PONDEROSA-C/S [22] assisted Xplor-NIH [23].

Statistics for the solution structure (Table 1) are indicative of its high quality. The average number of constraints per residue was 17.6, and, of these, an average of 4.2 per residue were long-range constraints. The root mean square deviation (rmsd) for backbone heavy atoms was< 1.0 Å overall and~0.6 Å for backbone heavy atoms in regular secondary structure. Of the

Table 1. Statistics Describing the NMR Solution Structure of Wild-type apo-CobY.

Constraints	Description	Value
	Conformationally restricting distance constraints (number)	
	Intraresidue [i = j]	1049
	Sequential [(i–j) = 1]	903
	Medium Range [1 < (i–j) ≤ 5]	470
	Long Range [(i–j) > 5]	824
	Total	3246
	Dihedral angle constraints (number)	
	φ	110
	ψ	110
	Constraints per residue (average number)	
	Total	17.6
	Long-range	4.2
	CYANA [18] target function (Å)	6.60+ 0.43
	Average rmsd to the mean coordinates of water refined CNS coordinates (Å)	
	regular secondary structure elements, backbone heavy	0.62±0.08 [a]
	regular secondary structure elements, all heavy atoms	0.94+0.08 [b]
	backbone heavy atoms	0.66±0.07 [b]
	all heavy atoms	1.05±0.09 [b]
Validation parameters	Description	
	PROCHECK [24] rawscore (φ and Ψ/all dihedral angles)	-0.7/-0.12 [c]
	PROCHECK Z-scores (φ and Ψ/all dihedral angles)	0.04/-0.71 [c]
	MOLPROBITY [25] raw score/Z-score	34.76/-4.44 [c]
	Ramachandran plot summary: ordered residue ranges (%)	
	most favored regions	91.5
	additionally allowed regions	8.2
	generously allowed regions	0.2
	Average number of distance constraint violations per CYANA conformer	
	0.2–0.5 Å	0.0
	> 0.5 Å	0.0
	Average number of dihedral-angle constraint violations per CYANA conformer	0.0

[a] Residues:2–7 (β1), 22–24, 27–29, 29–39(α1), 44–49 (β2), 54–64 (α2), 70–74 (β3), 80–90 (α3), 95–99 (β4), 101–104, 107–123 (α4), 129–135(β5), 149–157(β6), 166–170(β7), 175–177, 181–195 (α5).

[b] Residues: 2–7, 21–135, 148–195.

[c] Residues: 2–7, 20–25, 27–102, 106–139, 149–152, 154–160, 163–176, 179–194.

doi:10.1371/journal.pone.0141297.t001

backbone torsion angles, 91% were in the most favored and 8% were in additionally allowed regions of the Ramachandran plot. The PROCHECK [24] Z-scores for backbone / all atoms were−0.04/ −0.71.

The structure consists of a mixed α/β fold (Fig 2). The seven β-strands (A-G) consist of residues β_A(D2–M6), β_B(N44–T49), β_C(I70–D74), β_D(F95–S99), β_E(A129–M133), β_F(P151–V157), and β_G(E167–V170). The five α-helices (I-V) consist of residues α_I(L29–K39), α_{II}(P54–Y64), α_{III}(Y80–Y90), α_{IV}(K108–K123), and α_V(T180–K192). The orientations of the β-strands make up a twisted β-sheet (Fig 2A, 2B, and 2C); six of the seven β-strands are arranged in parallel fashion: $\beta_C(\uparrow)$ $\beta_B(\uparrow)$ $\beta_A(\uparrow)$ $\beta_D(\uparrow)$ $\beta_F(\downarrow)$ $\beta_E(\uparrow)$ $\beta_G(\uparrow)$. In addition, a short and stable β-hairpin is located between residues I22 and L29, and a short anti-parallel β-sheet-like structure is formed by residues D101-N104 and I175-N177. Four α-helices (I, II, IV, and V) are arranged on one side of the β-sheet, whereas one α-helix (IV) is on the other side of the β-sheet. α-Helix I is in contact with β-strands A and B, whereas α-helix II is in contact with β-strands B and C. α-helices I and II also contact one other; α-helix III contacts half of the β-sheet (β-strands C, B, A, D, and F); and α- helix IV contacts the other side of the β-sheet (β-strands A, D, F, E, and G). The loops connecting the secondary structural elements (α_1–β_A, α_4–β_D, β_E–β_F, and β_G–α_5) are highly flexible and unstructured. Resonance assignments could

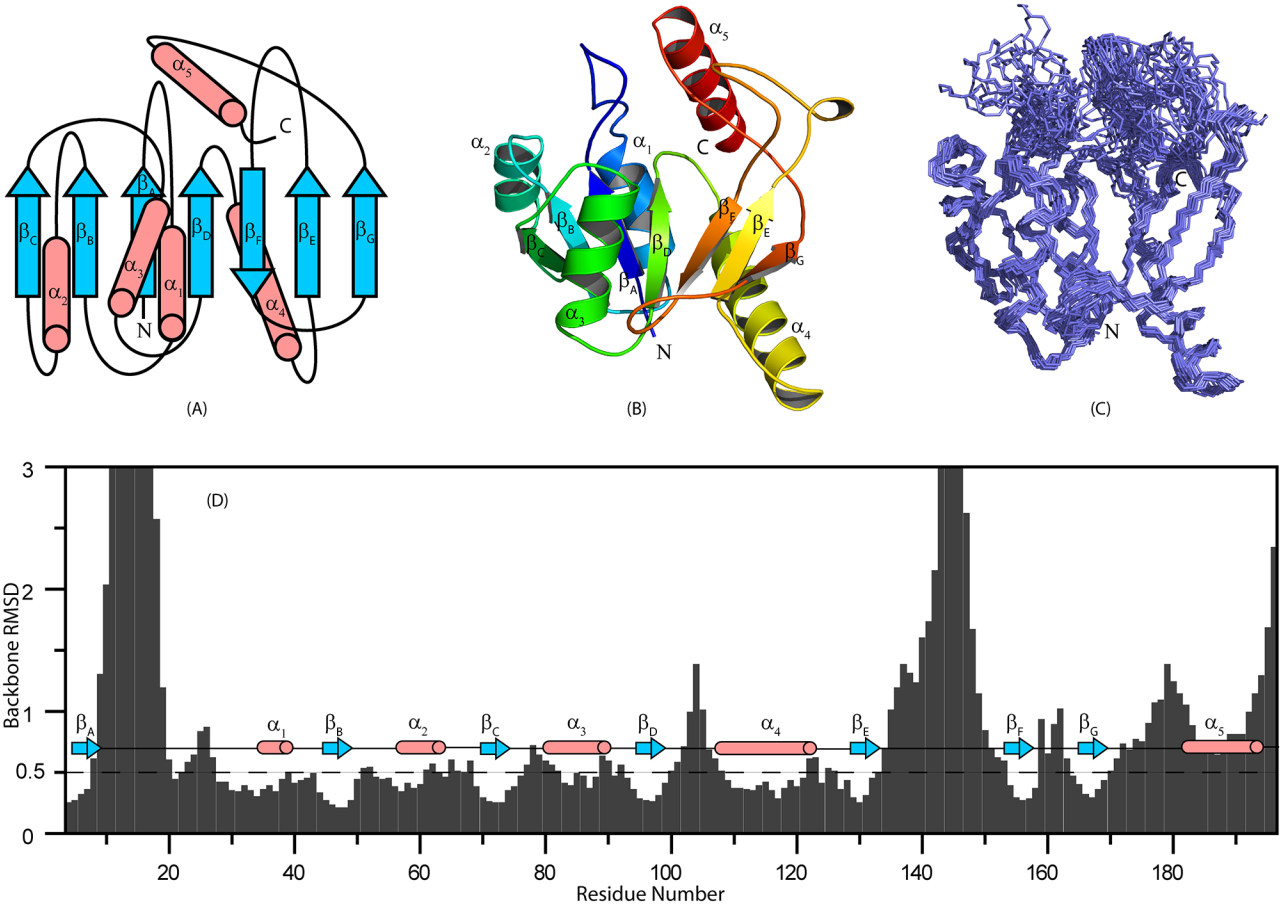

Fig 2. Three-dimensional Solution Structure of apo-free CobY. (A) Secondary structure topology representing seven β-stands and five α-helices. (B) Ribbon diagram of the lowest energy conformer of apo-CobY. (C) Overlay of the regular secondary structure of the 20 lowest energy conformers that showed the fewest violations in CYANA (N- and C-terminals are labeled). (D) The rmsd of the backbone atoms plotted against the corresponding amino acid number. Residues 10–20 and 135–150 displayed the highest rmsd values. Also shown are the positions of the α-helices and β-strands.

doi:10.1371/journal.pone.0141297.g002

not be obtained for residues in some of these loops because of exchange broadening, which led to the disappearance of the amide peaks. The backbone rmsd plotted against the amino acid sequence (Fig 2D) shows that the polypeptide chain is flexible between residues 8–20 and133–153. The C-terminal helix is also relatively dynamic as determined from heteronuclear NOE values. The coordinates were deposited in the Protein Data Bank (PDB) with accession code 2MZB, and the chemical shifts were deposited in Biological Magnetic Resonance Data Bank (BMRB) with accession code 25482.

Structural homologues of apo-CobY

We used the software programs DALI [26] and ProFunc [27] to search for structural homologues of apo-CobY. The five most similar structures, all determined by X-ray crystallography, contained mononucleotide binding domains with a canonical Rossmann fold (Fig 3). Cytidinyl monophosphate2-keto-3-deoxy-manno-octonic acid synthetase (CMP:Kdo) from *Escherichia coli* (PDB 1H7F, Z-score 15.8, rmsd 2.6 Å, seq ID 14%) is involved in the synthesis of lipopolysaccharides that are toxic to Gram-negative bacteria [28]. Glucose-1-phosphate cytidylyl

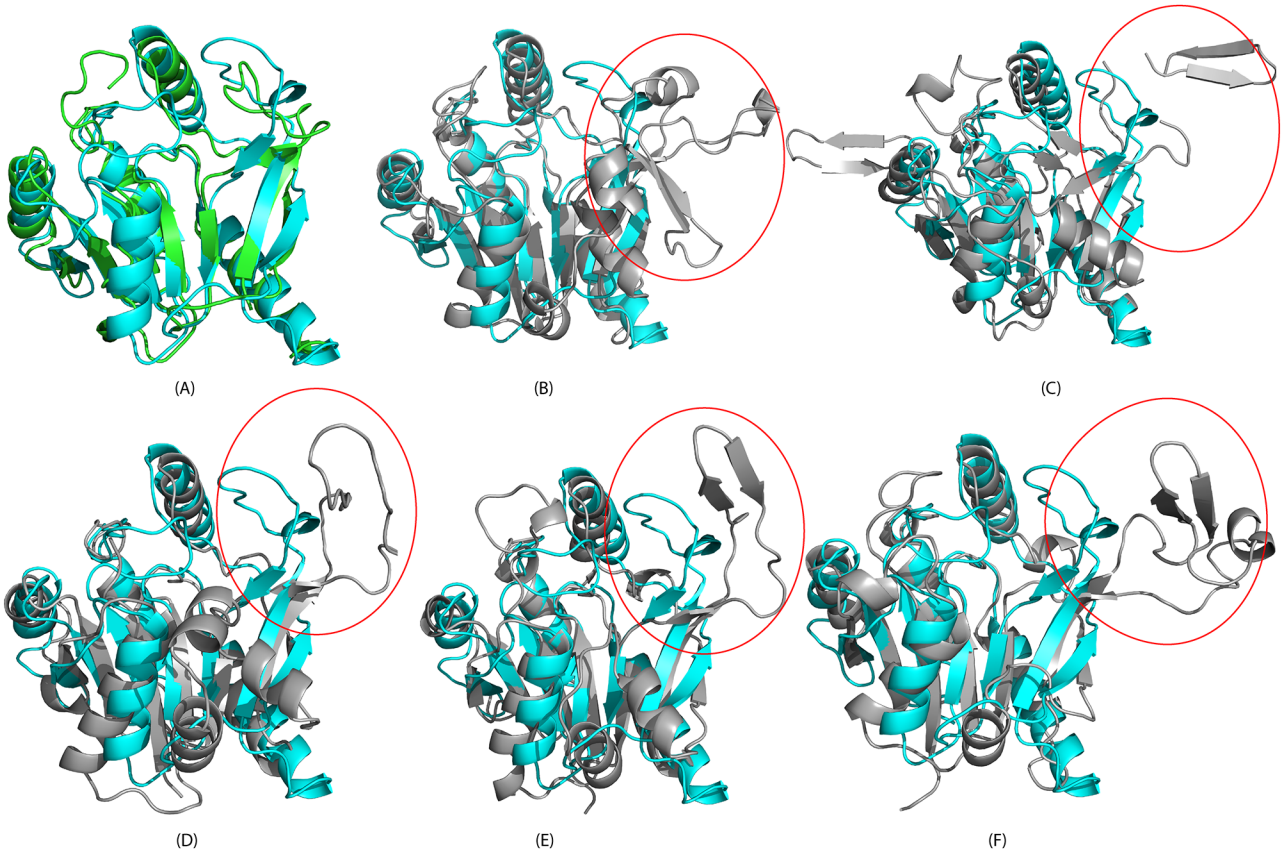

Fig 3. Overlay of the Ribbon Structure apo-CobY (cyan) with those of Structurally Similar Proteins. (A) (green) X-ray structure of the CobY^{G153D}:GTP complex (PDB 3RSB) (87% structural overlap with rmsd 1.82 Å; fragment/topology score 0.95/0.94 with match size 113). (B) (gray) X-ray structure of CMP:2-keto-3-deoxy-manno-octonic acid synthetase (PDB 1H7F).(75.5% structural overlap with rmsd 1.84 Å; fragment/topology score 0.93/1.0 with match size 148). (C) (gray) X-ray structure of α-D-glucose-1-phosphate cytidylyl transferase (PDB 1WVC) (75.5% structural overlap with rmsd 2.15 Å; fragment/topology score 0.86/1.0 with match size 148). (D) (gray) X-ray structure of acytidylyl transferase (PDB 2VSI) (74.5% structural overlap with rmsd 1.98 Å; fragment/topology score 0.91/1.0 with match size 146). (E) X-ray structure of 2-C-methyl-D-erythritol 4-phosphate cytidylyl transferase(PDB 1VPA) (73% structural overlap with rmsd 1.86 Å; fragment/topology score 0.91/1.0 with match size 143). (F) X-ray structure of CMP-acylneuraminate synthetase (PDB 1EYR) (70% structural overlap with rmsd 1.95 Å; fragment/topology score 0.88/1.0 with match size 137). PYMOL [20] was used to generate the structures, and the CLICK [33] program was used to carry out the pairwise alignments.

doi:10.1371/journal.pone.0141297.g003

transferase from *Salmonella typhi* (PDB 1WVC, Z-score 15.2, rmsd 3.3 Å, seq ID 18%) catalyzes the transfer of a CMP moiety from CTP to glucose 1-phosphate [29]. Cytidine transferase from *Streptococcus pneumonia* (PDB 2VSI, Z-score 15.6, rmsd 3.0 Å, seq ID 13%) is involved in the synthesis of cytidine-5'-diphosphate (CDP)-ribitol from ribitol 5-phosphate and CTP [30]. 2-C-methyl-D-erythritol 4-phosphate cytidylyl transferase from *Thermotoga maritima* (PDB 1VPA, Z-score 15.3, rmsd 3.1 Å, seq ID 18%) catalyzes the formation of 4-diphosphocytidyl-2-C-methyl-D-erythritol from CTP and 2-C-methyl-D-erythritol 4-phosphate. N-acylneuraminate cytidylyl transferase from *Neisseria meningitides* (PDB 1EYR, Z-score 15.3, rmsd 3.0 Å, seq ID 17%) catalyzes the reaction of CTP and N-acylneuraminate to form CMP-N-acylneuraminate and bisphosphate [31]. A structure-based multiple sequence alignment performed by PROMALS3D [32] revealed several highly-conserved residues (Fig 4): A3, I5, A7, R13, K19, G26, (K/R)27, (D/E)58, T180, D183, and L184. These residues appear to play important roles in nucleotide binding. In particular, residues R13 and K19 directly coordinate the phosphate group of GTP in the X-ray structure of CobY^{G153D} [8].

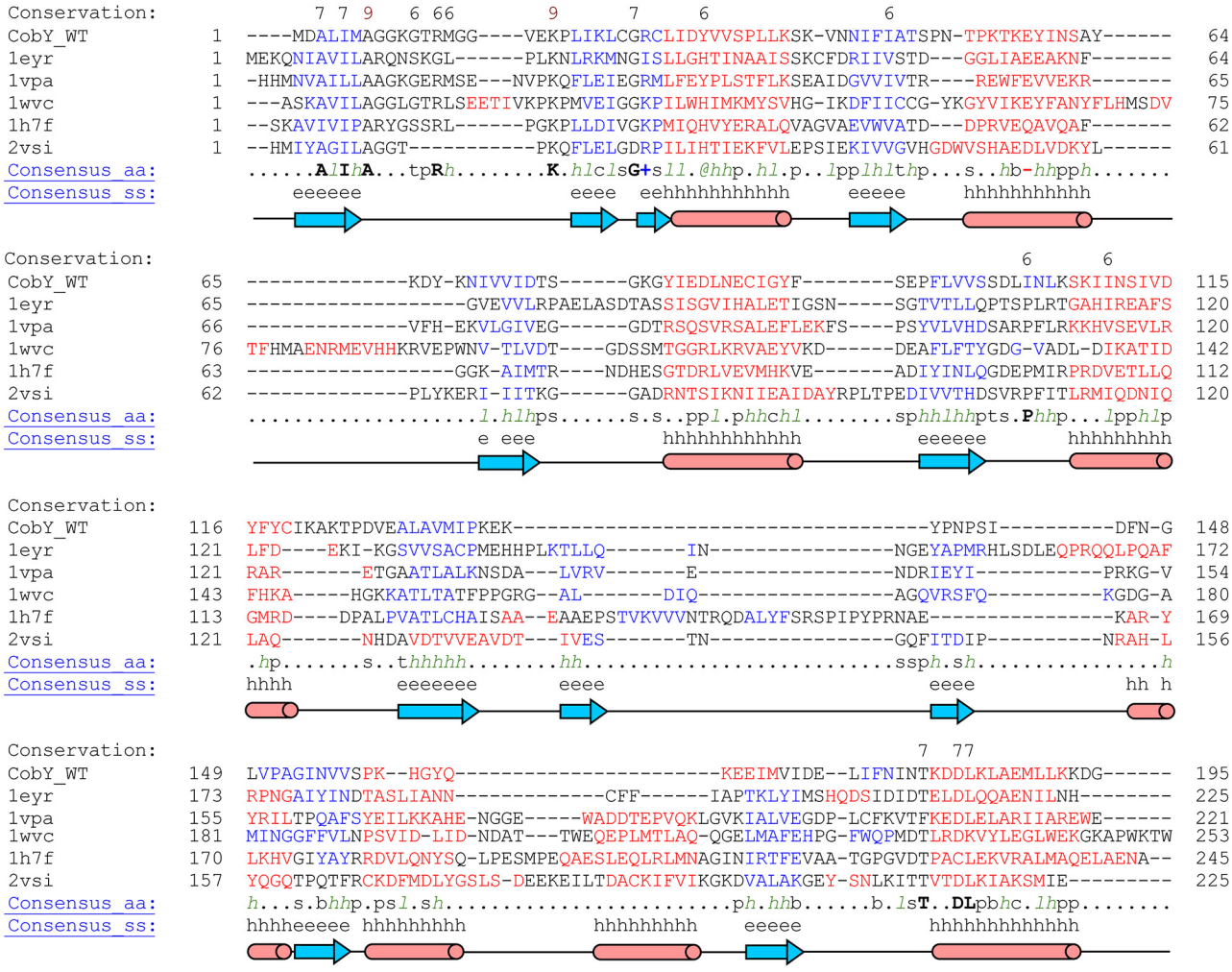

Fig 4. Structure-based Multiple Sequence Alignment of Wild-type apo-CobY with the Five Most Structurally Similar Proteins. The alignment, which was carried out using the PROMALS3D program [32], shows substantial sequence alignment of secondary structural elements derived from the 3D structures: (blue) α-helix; (red) β-strand.

doi:10.1371/journal.pone.0141297.g004

All these structures share < 20% sequence identity with CobY and additionally contain HTH motifs and/or a β-hairpin structure that facilitates the formation of homodimers (Fig 4).

Dynamics of ligand free CobY

One of the advantages of NMR spectroscopy over X-ray crystallography is its ability to provide information about the dynamic properties of proteins in solution. For CobY we accomplished this by measuring nitrogen spin-lattice (T_1) and spin-spin (T_2) relaxation times and heteronuclear NOEs (^{15}N NOEs) for backbone amide resonances. As shown in Fig 5, we found that the relaxation parameters are fairly similar throughout the polypeptide chain, indicating uniform overall protein dynamics. The only exceptions were inflexible loops connecting regular secondary structure elements, in particularα_1-β_A, α_4-β_D, β_E-β_F, and β_G-α_5; these regions yielded weak electron density in the X-ray studies of CobY. The average T_1 (~750 ms) and T_2 (~70 ms)values are those expected for a monomeric protein of ~23 kDa and are consistent with the 3D NMR solution structure. In addition, the rotational correlation times (τ_c) of the amide protons calculated from T_1 and T_2 revealed an average τ_c = 9.9 ± 0.7 ns (Fig 5) consistent with monomeric protein in solution. By contrast, the X-ray structure of the CobY^{G153D}:GTP complex was modeled as a weak dimer [8].

Comparison of the NMR structure of apo-CobY and the X-ray structure of the CobY^{G153D}:GTP complex

The solution structure of apo-CobY and the crystal structure of CobY^{G153D}:GTP complex(PDB 3RSB) [8] exhibit similar 3D folds (structures superimposed in Fig 6A). The elements of regular secondary structure (consisting of 67 amino acid residues) superimposed with an average rmsd = 0.83Å. The X-ray structure has a relatively low resolution (2.8 Å), and electron density was not identified for residues 8–11, 74–81, 126–127, and 192–196. Perhaps the largest structural differences are in α-helix-III, which is structured in the NMR solution structure but unstructured in the X-ray structure (Fig 6B). Although isothermal titration calorimetry (ITC) studies suggested one GTP molecule per two units of CobY [9], the X-ray structure of the CobY^{G153D}:GTP complex was modeled as a dimer with one GTP molecule bound to each subunit. The ITC results were obtained with active enzyme that may have been turning over during the experiment. Our NMR experiments with both CobY and CobY^{G153D} are consistent with a 1:1 complex.

Complex formation of CobY with GTP

To probe the effect of added GTP on apo-CobY, we titrated a sample of ^{15}N-labeled apo-CobY with GTP and followed the chemical shifts in a series of ^{1}H-^{15}NHSQC spectra. Several amide cross peaks exhibited large perturbations (Fig 6D–6F), indicating that significant conformational changes accompanied the formation of the GTP complex. ^{1}H-^{15}N HSQC spectra acquired following the addition sub-stoichiometric amounts of GTP (not shown), exhibited two sets of peaks, one corresponding to free CobY and one to the CobY:GTP complex; this indicates a slow off rate for GTP dissociation.

Two factors appear to be responsible for these chemical shift changes: (i) GTP-induced ordering of the binding domain and (ii) electrostatic interactions between the ligand and protein backbone. In the X-ray structure of the CobY^{G153D}: GTP complex, the tri-phosphate group of GTP is in the proximity of the region of the protein (residues 10–18) that appears disordered in the apo-enzyme both in X-ray crystal data, which lacked electron density for these residues, and in the solution spectra, which lacked signals from these residues as attributed to exchange broadening. The overlaid expansions of three regions of the ^{15}N HSQC spectra of

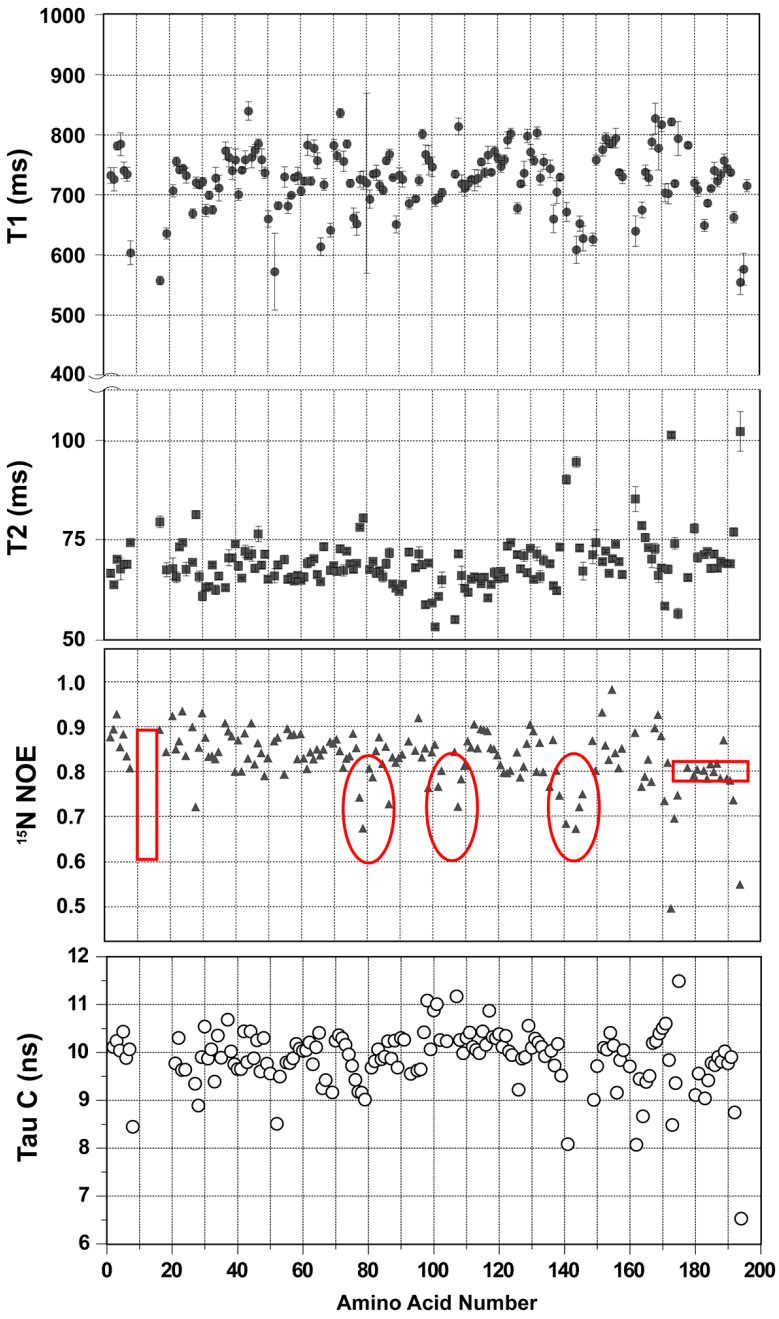

Fig 5. Dynamics of apo-CobY as Represented by Residue-specific Backbone Amide Spin-lattice (T_1) and Spin-spin (T_2) Relaxation Times, Heteronuclear NOE (^{15}N NOE) Values, and Correlation Times. The flexible regions of the polypeptide chain are circled in red; the vertical red box represents missing resonances from residues that are assumed to be flexible; and the horizontal red box indicates the C-terminal helix, which appears to be more flexible than other secondary features as indicated by the smaller ^{15}N NOE values. The τ_c values were calculated from measured T_1 and T_2 values by using the formula, $\tau_c = 1/4\pi\nu_N (\sqrt{6}(T1/T2) - 7)$. The average τ_c value (9.9 ± 0.7 ns) indicates that CobY is monomeric in solution under the NMR sample conditions.

doi:10.1371/journal.pone.0141297.g005

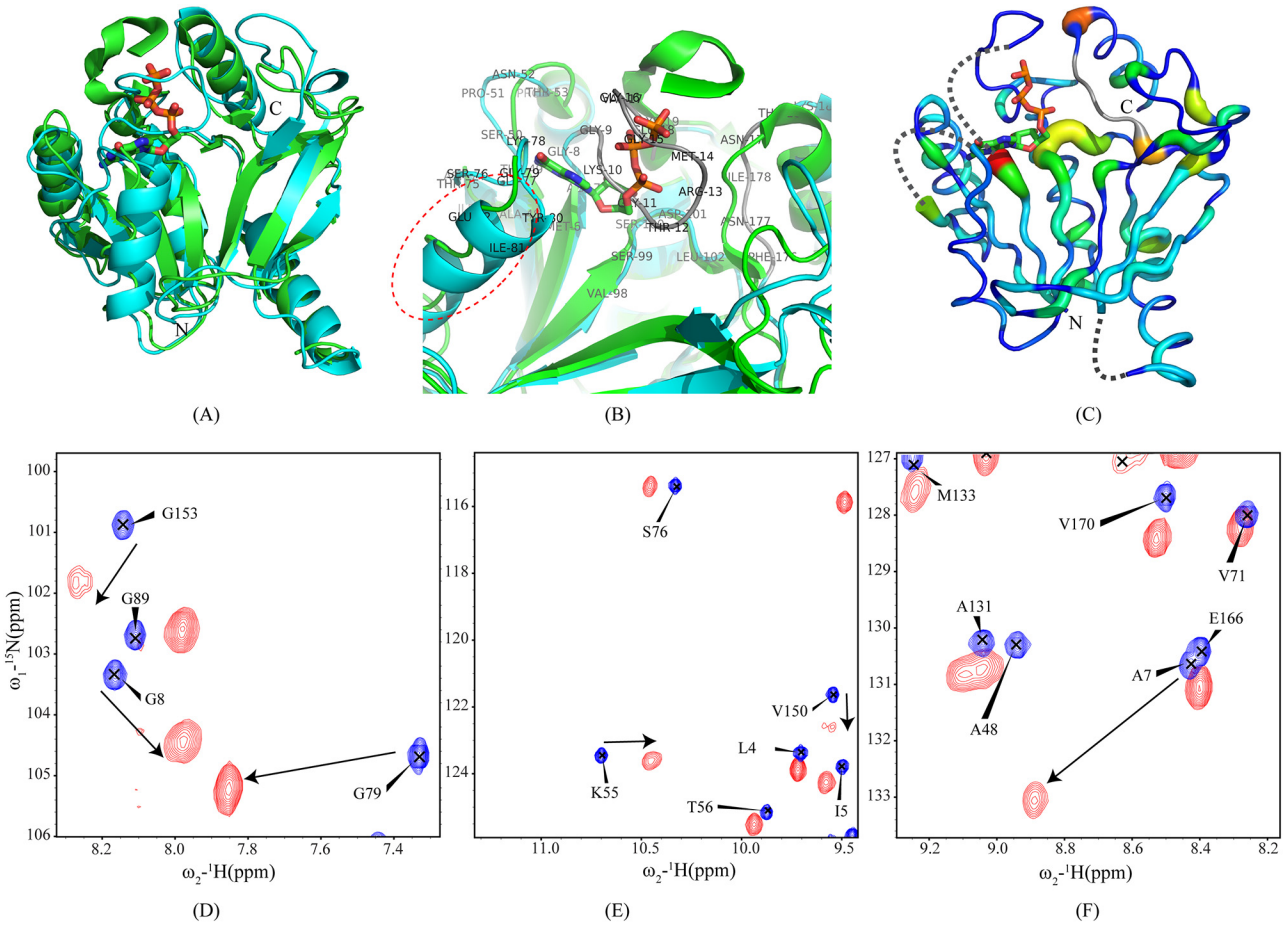

Fig 6. Comparison of Structures of apo-CobY and CobY^{G153D}:GTP Complex and Comparison of ^{1}H-^{15}N HSQC Spectra of CobY and CobY:GTP. (A) Superposition of the 3D structures of apo-CobY determined by NMR (cyan) and CobY^{G153D}:GTP determined by X-ray crystallography (green) with the GTP displayed as a stick model. (B) Expansion of the overlaid structures showing the GTP binding site. Residues perturbed upon complex formation with GTP are annotated. Whereas α-helix-III (circled in red) is well defined in the structure of apo-CobY, it is poorly resolved in the X-ray structure of the complex. (C) Weighted rmsd chemical shift differences ($[0.5[\Delta\delta(^1H^N)^2+ (0.2\Delta\delta(^{15}N))^2]]^{1/2}$) between apo-CobY and CobY:GTP mapped onto the X-ray structure of CobY^{G153D}:GTP. The magnitude of the shift is coded by a spectrum with red largest shift and blue small or no shift. Residues not detected or assigned in both NMR in the spectra compared are shown in gray. The dotted regions of the polypeptide chain represent ones for which no electron density was detected (D-F) Overlays of three regions of the ^{15}N HSQC spectra of CobY (blue) and CobY:GTP (red). The cross peaks from CobY are annotated with their assignments, and the arrows indicate the changes in peak positions upon complex formation with GTP.

doi:10.1371/journal.pone.0141297.g006

CobY and CobY:GTP complex (Fig 6D–6F) indicate that the amide protons of A7, G8, K55, G79, G153 shift significantly upon GTP binding. The weighted chemical shift perturbations (CSPs) mapped on 3D structure of CobY^{G153D} (Fig 6C) show that some are close to the GTP binding site and others are distant.

Comparison of CobT and CobY^{G153D}

Comparison of the ^{1}H-^{15}N HSQC spectra of [U-^{15}N]-CobY and [U-^{15}N]-CobY^{G153D} (Fig 7A) indicates that the chemical shift differences are small. The sample of ^{15}N-labeled CobY^{G153D} was saturated with GTP, and the resulting spectrum was compared to that of apo-CobY^{G153D} (Fig 7B). The chemical shift perturbations upon GTP binding are very similar to those observed with wild-type CobY (Fig 1B).

The differences in the chemical shifts of CobY and CobY^{G153D} are plotted as a function of residue number in Fig 8A and are mapped onto the 3D structure of the protein in Fig 8B. As

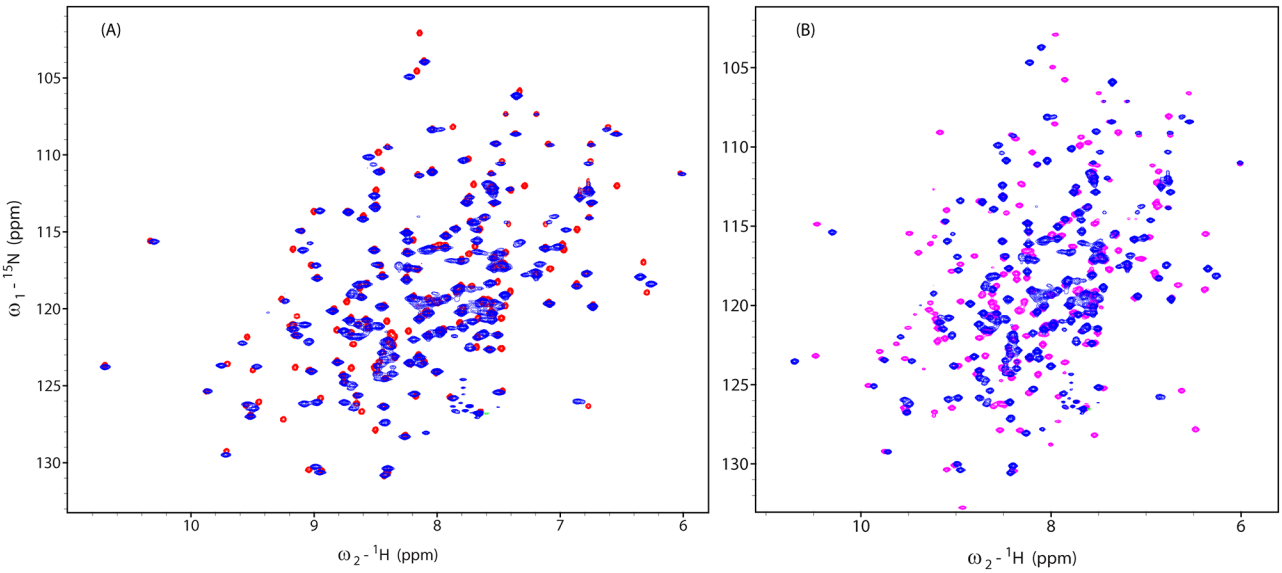

Fig 7. Comparison of ^{1}H-^{15}N HSQC Spectra of CobY and CobYG153D. (A) Spectrum of apo-CobY (red) overlaid with that of apo-CobYG153D(blue). (B) Spectrum of apo-CobYG153D (blue) overlaid with that of the CobYG153D:GTP complex (purple).

doi:10.1371/journal.pone.0141297.g007

expected, atoms in residues near residue 153 (the substitution site) exhibit the largest chemical shift differences.

The GTP complexes with wild-type CobY and CobY^{G153D} proved to be unstable in solution. NMR spectra taken over time (not shown) indicated each complex converted to an unknown intermediate state over a period of about 24 hours (most probably the "switch-off" GDP

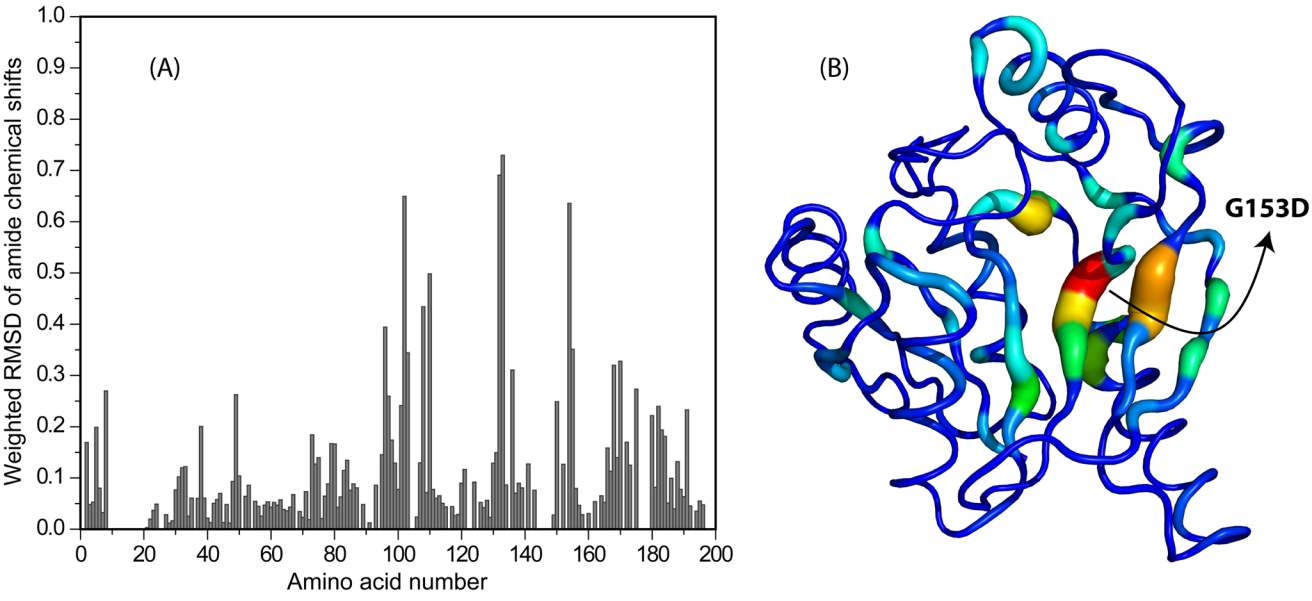

Fig 8. Representation of Differences in the Chemical Shifts of CobY and CobY^{G153D}. (A) Weighted rmsd of amide proton chemical shift differences ([0.5 [$\Delta\delta(^1H^N)^2$+ (0.2$\Delta\delta(^{15}N))^2$]]$^{1/2}$) plotted as a function of the amino acid residue number. (B) Mapping of the weighted rmsd chemical shift differences onto the 3D NMR structure of CobY. Color code: (red, yellow, green, cyan) spectrum of chemical shift differences from largest to small; (blue) no significant chemical shift difference.

doi:10.1371/journal.pone.0141297.g008

complex) and then converted over a period of days to species with spectra resembling those of the apo-proteins. Repeated attempts to make a stable GTP-CobY complex by reducing the temperature and saturating with GTP were unsuccessful. The instability of the complexes prevented us from determining their solution structures.

Conclusions

Solution NMR studies of apo-CobY yielded a 3Dstructure of high quality with a fold is similar to that of the low resolution X-ray structure of the $CobY^{G153D}$:GTP complex [8]. We found CobY to be monomeric in solution in both its apo- and GTP-bound forms, whereas the X-ray structure of the $CobY^{G153D}$:GTP complex was modeled as a homodimer. Other differences may reflect problems in tracing the chain in the X-ray map.

It is known that complexes of GTPases with GTP are conformationally flexible to allow for the conversion of GTP to GDP and transfer of the phosphate group. The proposed two-state mechanism has been extensively studied for small GTPases, such as Ras, RhoA, and Sec4 [34]. The active "switch-on" state has GTP bound, whereas the inactive "switch-off" state has GDP bound. Titration studies of CobY followed by NMR spectroscopy revealed that CobY forms a tight 1:1 complex with GTP. However, the complex was found to degrade over time, which prevented the determination of its solution structure.

Acknowledgments

The authors thank Woonghee Lee for performing water refinement of the structure by PONDOROSA C/S assisted XPLOR-NIH. KKS thanks Dr. Jagadeesh, Dr. Kunwar, and the Director-CSIR-IICT for their support and encouragement

Author Contributions

Conceived and designed the experiments: KKS MO WMW JCE-S. Performed the experiments: KKS MO MT WMW. Analyzed the data: KKS MT. Wrote the paper: KKS MO MT WMW JCE-S JLM.

References

1. Battersby AR. Tetrapyrroles: the pigments of life. Nat Prod Rep. 2000; 17(6):507–26. PMID: 11152419.
2. Chan CH, Escalante-Semerena JC. ArsAB, a novel enzyme from *Sporomusa ovata* activates phenolic bases for adenosylcobamide biosynthesis. Mol Microbiol. 2011; 81(4):952–67. doi: 10.1111/j.1365-2958.2011.07741.x PMID: 21696461; PubMed Central PMCID: PMC3182833.
3. O'Toole GA, Escalante-Semerena JC. Purification and characterization of the bifunctional CobU enzyme of *Salmonella typhimurium* LT2. Evidence for a CobU-GMP intermediate. J Biol Chem. 1995; 270(40):23560–9. PMID: 7559521.
4. Thomas MG, Thompson TB, Rayment I, Escalante-Semerena JC. Analysis of the adenosylcobinamide kinase/adenosylcobinamide-phosphate guanylyltransferase (CobU) enzyme of Salmonella typhimurium LT2. Identification of residue His-46 as the site of guanylylation. J Biol Chem. 2000; 275 (36):27576–86. doi: 10.1074/jbc.M000977200 PMID: 10869342.
5. Thompson TB, Thomas MG, Escalante-Semerena JC, Rayment I. Three-dimensional structure of adenosylcobinamide kinase/adenosylcobinamide phosphate guanylyltransferase from *Salmonella typhimurium* determined to 2.3 Å resolution. Biochemistry. 1998; 37(21):7686–95. doi: 10.1021/bi973178f PMID: 9601028.
6. Thomas MG, Escalante-Semerena JC. Identification of an alternative nucleoside triphosphate: 5'-deoxyadenosylcobinamide phosphate nucleotidyltransferase in *Methanobacterium thermoautotrophicum* delta H. J Bacteriol. 2000; 182(15):4227–33. PMID: 10894731; PubMed Central PMCID: PMC101920.
7. Thompson TB, Thomas MG, Escalante-Semerena JC, Rayment I. Three-dimensional structure of adenosylcobinamide kinase/adenosylcobinamide phosphate guanylyltransferase (CobU) complexed with GMP: evidence for a substrate-induced transferase active site. Biochemistry. 1999; 38(40):12995–3005. PMID: 10529169.

8. Newmister SA, Otte MM, Escalante-Semerena JC, Rayment I. Structure and mutational analysis of the archaeal GTP:AdoCbi-P guanylyltransferase (CobY) from Methanocaldococcus jannaschii: insights into GTP binding and dimerization. Biochemistry. 2011; 50(23):5301–13. doi: 10.1021/bi200329t PMID: 21542645; PubMed Central PMCID: PMC3125946.

9. Otte MM, Escalante-Semerena JC. Biochemical characterization of the GTP:adenosylcobinamide-phosphate guanylyltransferase (CobY) enzyme of the hyperthermophilic archaeon *Methanocaldococcus jannaschii*. Biochemistry. 2009; 48(25):5882–9. doi: 10.1021/bi8023114 PMID: 19489548; PubMed Central PMCID: PMC2757067.

10. Zhao Q, Frederick R, Seder K, Thao S, Sreenath H, Peterson F, et al. Production in two-liter beverage bottles of proteins for NMR structure determination labeled with either ^{15}N- or ^{13}C-^{15}N. J Struct Funct Genomics. 2004; 5(1–2):87–93. PMID: 15263847.

11. Delaglio F, Grzesiek S, Vuister GW, Zhu G, Pfeifer J, Bax A. NMRPIPE—A Multidimensional Spectral Processing System Based on UNIX Pipes. J Biomol NMR. 1995; 6(3):277–93. 806. PMID: 8520220

12. Bartels C, Xia TH, Billeter M, Güntert P, Wüthrich K. The Program XEASY for Computer-Supported NMR Spectral-Analysis of Biological Macromolecules. J Biomol NMR. 1995; 5:1–10. .

13. Lee W, Tonelli M, Markley JL. NMRFAM-SPARKY: enhanced software for biomolecular NMR spectroscopy. Bioinformatics. 2014. doi: 10.1093/bioinformatics/btu830 PMID: 25505092.

14. Bahrami A, Assadi AH, Markley JL, Eghbalnia HR. Probabilistic interaction network of evidence algorithm and its application to complete labeling of peak lists from protein NMR spectroscopy. PLoS Comput Biol. 2009; 5(3):e1000307. Epub 2009/03/13. doi: 10.1371/journal.pcbi.1000307 PMID: 19282963; PubMed Central PMCID: PMCPMC2645676.

15. Sattler M, Schleucher J, Griesinger C. Heteronuclear Multidimensional NMR Experiments for the Structure Determination of Proteins in Solution Employing Pulsed Field Gradients. Prog Nucl Mag Res Sp. 1999; 34(2):93–158. .

16. Kanelis V, Farrow NA, Kay LE, Rotin D, Forman-Kay JD. NMR studies of tandem WW domains of Nedd4 in complex with a PY motif-containing region of the epithelial sodium channel. Biochem Cell Biol. 1998; 76(2–3):341–50. PMID: 9923703.

17. Shen Y, Delaglio F, Cornilescu G, Bax A. TALOS+: a hybrid method for predicting protein backbone torsion angles from NMR chemical shifts. J Biomol NMR. 2009; 44(4):213–23. Epub 2009/06/24. doi: 10.1007/s10858-009-9333-z PMID: 19548092; PubMed Central PMCID: PMC2726990.

18. Güntert P. Automated NMR structure calculation with CYANA. Methods Mol Biol. 2004; 278:353–78. .

19. Koradi R, Billeter M, Wüthrich K. MOLMOL—A Program for Display and Analysis of Macromolecular Structures. J Mol Graph. 1996; 14(1):51–5. .

20. DeLano WL, Lam JW. PyMOL: A communications tool for computational models. Abstr Pap Am Chem S. 2005; 230:U1371–U2. ISI:000236797302763.

21. Bhattacharya A, Tejero R, Montelione GT. Evaluating protein structures determined by structural genomics consortia. Proteins. 2007; 66(4):778–95. Epub 2006/12/23. doi: 10.1002/prot.21165 PMID: 17186527.

22. Lee W, Stark JL, Markley JL. PONDEROSA-C/S: client-server based software package for automated protein 3D structure determination. J Biomol NMR. 2014; 60(2–3):73–5. doi: 10.1007/s10858-014-9855-x PMID: 25190042; PubMed Central PMCID: PMCPMC4207954.

23. Schwieters CD, Kuszewski JJ, Tjandra N, Clore GM. The Xplor-NIH NMR molecular structure determination package. J Magn Reson. 2003; 160(1):65–73. .

24. Laskowski RA, MacArthur MW, Moss DS, Thornton JM. PROCHECK: A Program to Check the Stereochemical Quality of Protein Structures. J Appl Cryst. 1993; 26(Part II):283–91. doi: 10.1107/S0021889892009944 .

25. Chen VB, Arendall WB 3rd, Headd JJ, Keedy DA, Immormino RM, Kapral GJ, et al. MolProbity: all-atom structure validation for macromolecular crystallography. Acta Crystallogr D Biol Crystallogr. 2010; 66(Pt 1):12–21. Epub 2010/01/09. doi: 10.1107/S0907444909042073 PMID: 20057044; PubMed Central PMCID: PMC2803126.

26. Holm L, Sander C. Dali—a Network Tool for Protein-Structure Comparison. Trends Biochem Sci. 1995; 20(11):478–80. .

27. Laskowski RA, Watson JD, Thornton JM. ProFunc: a server for predicting protein function from 3D structure. Nucleic Acids Res. 2005; 33(Web Server issue):W89–93. doi: 10.1093/nar/gki414 PMID: 15980588; PubMed Central PMCID: PMC1160175.

28. Jelakovic S, Schulz GE. The structure of CMP:2-keto-3-deoxy-manno-octonic acid synthetase and of its complexes with substrates and substrate analogs. J Mol Biol. 2001; 312(1):143–55. doi: 10.1006/jmbi.2001.4948 PMID: 11545592.

29. Koropatkin NM, Cleland WW, Holden HM. Kinetic and structural analysis of alpha-D-Glucose-1-phosphate cytidylyltransferase from *Salmonella typhi*. J Biol Chem. 2005; 280(11):10774–80. doi: 10.1074/jbc.M414111200 PMID: 15634670.

30. Baur S, Marles-Wright J, Buckenmaier S, Lewis RJ, Vollmer W. Synthesis of CDP-activated ribitol for teichoic acid precursors in *Streptococcus pneumoniae*. J Bacteriol. 2009; 191(4):1200–10. doi: 10.1128/JB.01120-08 PMID: 19074383; PubMed Central PMCID: PMC2631998.

31. Mosimann SC, Gilbert M, Dombroswki D, To R, Wakarchuk W, Strynadka NC. Structure of a sialic acid-activating synthetase, CMP-acylneuraminate synthetase in the presence and absence of CDP. J Biol Chem. 2001; 276(11):8190–6. doi: 10.1074/jbc.M007235200 PMID: 11113120.

32. Pei J, Tang M, Grishin NV. PROMALS3D web server for accurate multiple protein sequence and structure alignments. Nucleic Acids Res. 2008; 36(Web Server issue):W30–4. doi: 10.1093/nar/gkn322 PMID: 18503087; PubMed Central PMCID: PMC2447800.

33. Nguyen MN, Tan KP, Madhusudhan MS. CLICK—topology-independent comparison of biomolecular 3D structures. Nucleic Acids Res. 2011; 39(Web Server issue):W24–8. doi: 10.1093/nar/gkr393 PMID: 21602266; PubMed Central PMCID: PMC3125785.

34. Rao ST, Rossmann MG. Comparison of super-secondary structures in proteins. J Mol Biol. 1973; 76 (2):241–56. PMID: 4737475.